Dual-Band Dipole Antenna on an EBG Substrate for 5G Sub-6 GHz Wireless Communication Applications

S. Said [1, 2, *], A. Es-salhi [1], K. Kassmi[3], A. Messaoudi [3], A. Kaabal [4], E. Baghaz [5], and A. Faize [6]

[1] Departments of Physics, Research Center, High Studies of Engineering School, EHEI, Oujda, Morocco
[2]Department of Physics, Faculty of Sciences, University of Mohamed Premier, Oujda, Morocco
[3] Departments of Physics, Superior School of Technology, University of Mohamed Premier, Oujda, Morocco
[4] Departments of Physics, Faculty of Sciences and Techniques, Abdelmalek Essaâdi University, Al-Hoceima, Morocco
[5] Laboratory of Electronics, Instrumentation and Energetic, Department of physics, Faculty of Sciences, ChouaïbDoukkali University, El Jadida, Morocco
[6]Department of Physics, Polydisciplinary Faculty, University of Mohamed Premier, Nador, Morocco
*Correspondence: said.sara63@gmail.com (S.S.)

***Abstract*—With the increasing proliferation of communication devices and modern technologies, compactness has become a critical concern in antenna system design. Utilizing structures to reduce the size of antennas while preserving their performance characteristics is a complex challenge that requires a multidisciplinary approach. Traditional antennas operate by leveraging the electromagnetic properties of materials and specific geometries to emit or capture radio waves. However, these conventional antennas are often ill-suited for compact devices. One of the innovative approaches to address this issue is presented in this paper, which involves in the application of electromagnetic band gap structures below a half-wave dipole antenna appropriate for wireless communication systems. Using the electromagnetic bandgap structures and the superstrate results in an additional frequency descent of the dipole antenna, simultaneously, it allows to operate on the 2.6 and 3.5 GHz bands with a single antenna and also improves its performance (gain, directivity, antenna efficiency). Due to the use of the electromagnetic band gap structure in the proposed structure, the return loss of the dipole antenna is very low and the efficiency of the antenna is improved. Additionally, this technique reduces the antenna profile by 32%. At first the antenna operates in a 3.5 GHz frequency range, by introducing the electromagnetic bandgap structures, it operates in two frequency bands at 2.6 GHz and 3.5 GHz, appropriate to 5G applications. This antenna configuration is realized and measured to validate our simulation design.**

***Keywords*—electromagnetic band gap, radiation pattern, dual-band dipole antenna**

I. Introduction

Antenna design has advanced enormously over the past few decades and continues to undergo monumental development. Today's antenna design has seen new developments in technology, of which the discovery of Electromagnetic Band Gap (EBG) structures represents an important advance which have been proposed to address some of the antenna problems in wireless communications, especially increasing the antenna directivity and reducing its size and side lobes.

The birth of Electromagnetic Band Gap structures (EBG) comes from the optics area [1], known as photonic crystals in this domain. The Bragg mirror was elaborated in 1915 [2]. It reflects more than 99.5% of the incident energy due to constructive interference phenomena, which no other mirror can achieve. However, the incident wave and the normal incidence must be closely spaced. In 1987, Eli Yablonovitch extended the two and three dimensional Bragg mirrors concept for any incidence and for microwaves frequencies.

These structures are dielectric or metallic structures made of an assembly of periodic materials in one, two or three dimensions. having a band of prohibited frequency where no electromagnetic wave can propagate. They control electromagnetic wave propagation, and also frequency and spatial filtering.

Various scientific research activities in the telecommunications field, particularly in the electromagnetic field, focused on EBG structures that are extensively employed for several applications such as surface wave suppression for diverse designs of antennas, antenna gain enhancement and back lobe reduction [3, 4], Besides, they are employed for reducing the level of mutual coupling [5–7], efficient low profile wire antenna design [8, 9], miniaturized antenna design [12, 13], and the high gain antenna concept [14]. In this paper, it is proposed to integrate the EBG structures with the dipole antenna, which creates a new frequency in the lower frequency range of the antenna and enhances the antenna gain and directivity while reducing its size by about 32%. Recently, as mentioned in [15–17], miniaturized multiband antennas are obtained with several techniques,

Manuscript received May 20, 2023; revised June 22, 2023; accepted August 3, 2023.

the multiband antenna structure as mentioned generally supports a selective frequency band.

In this paper, instead, the antenna simultaneously functions in both 2.6 and 3.5 GHz bands, while maintaining the smallest size, using the technique of EBG structure. Therefore, this technique was chosen. The most original feature of this work is the simultaneous application of both frequency bands (2.6GHz, 3.5GHz), and a very important reduction in the size of the antenna. The proposed structure is realized experimentally and compared with the simulation results.

This paper is prepared as follows: the simulation results of an antenna with and without EBG structure is presented in Sections II. Section III is dedicated to the realization and measurement of the antenna, while the conclusion is provided in Section IV.

II. Structural Comparison for Antenna

A. Design of the Dipole Antenna

In 1886, Heinrich [18] developed the dipole antenna which is the simplest to study analytically and is the easiest to manufacture, it is composed of two metallic rods, fed in their middle and designed for transmitting or receiving electromagnetic radiation. In fifth generation (5G) wireless communication systems, the application of EBG structures has attracted much attention. This dipole antenna is optimized for operation around 3.5 GHz, its geometry is presented. in Fig. 1.It is made with two copper rods of length l=38.84mm and width e=1mm, its input impedance is 73 ohms. For a thin dipole antenna, when dipole length L is λ/2 (half wave dipole), the dipole antenna is in resonance, so its resonant frequency is equal to:

$$L = \frac{\lambda}{2} \leftrightarrow f = \frac{C}{2L} \quad (1)$$

S-parameter simulation results obtained, shown in Fig. 2, show a high resonant frequency around 3.5 GHz with a reflection coefficient lower than −35 dB, as well as a large bandwidth of about 580 MHz.

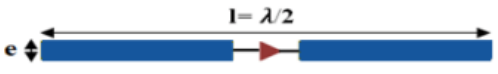

Figure 1. Half wave dipole antenna.

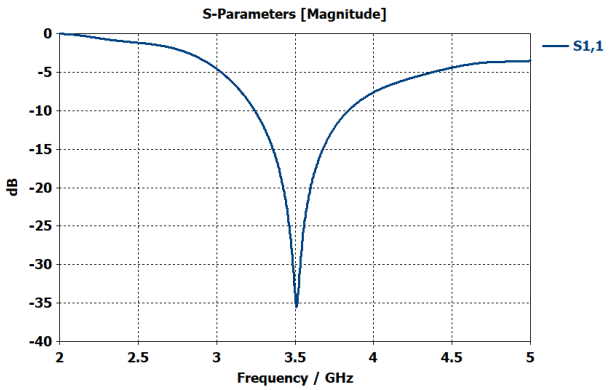

Figure 2. Half-wave dipole antenna S-parameters.

B. EBG Structure

The slotted EBG structure model used within this paper is the SHI (High Impedance Surface) structure. The SHI is a new type of electromagnetic bandgap structure designed by inserting slots in the conventional mushroom like EBG metal plates, as illustrated in Fig. 3.On the one hand, these slots influence the distribution of the current on surface plates, resulting in a longer current path, on the other hand, they create an additional capacitance between edges of the slots.

We have designed a new slotted EBG structure with three square of size 0.8mm ×0.8mm and a square ring of size width 0.3 mm positioned on a substrate Rogers RO3010, its thickness and relative permittivity are 1.27 mm and 10.2 mm respectively. Due to excellent mechanical and electrical stability of Rogers RO3010 and their competitive price, the material can be applied in various applications in a large frequency range. Such material characteristics make the Rogers RO3010 an excellent product for circuit miniaturization. The EBG structure unit cell is presented in Fig. 4, while its parametric value summary is presented in Table I.

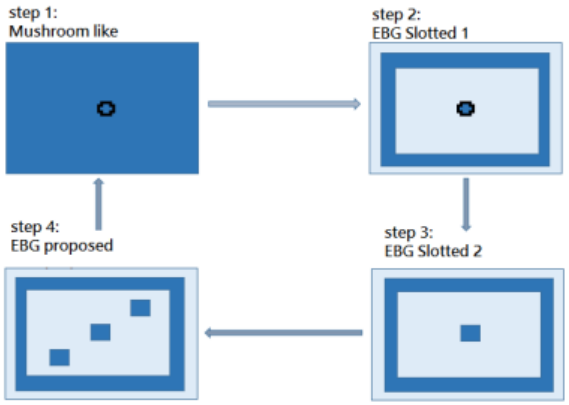

Figure 3. EBG unit cell design steps.

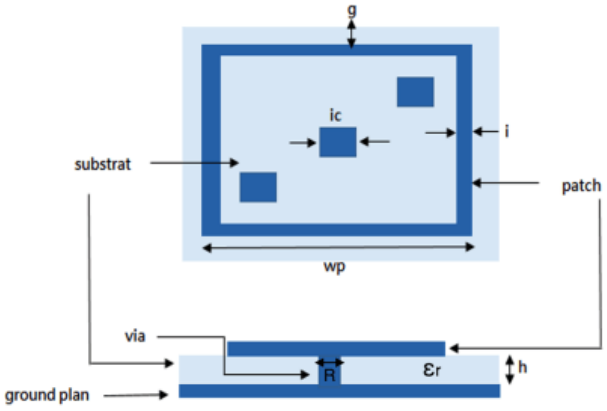

Figure 4. Unit cell EBG.

TABLE I. Unit Cell EBG Dimension (in mm)

Parameters	ic	I	G	Wp	h	M	R
Valeurs (mm)	0.8	0.3	0.2	6.4	1.27	0.0175	0.5

Various methods to analyze the characteristics of the SHI structure have been used. These methods can be categorized into three models: an equivalent circuit based model [19, 1], a transmission line model [20, 21], and a periodic boundary condition model [22]. The equivalent circuit model is considered the simplest to represent the SHI as a resonant circuit LC. SHI geometry is used for determining the capacitance C and inductance L values, while SHI resonant behavior is used for explaining the SHI structure's band gap characteristic. This model is simple to understand, however the approximation of L and C leads to poorly accurate results. The mechanism of the SHI structure is explained in Fig. 5. The inductance L is formed by the current flow through the metallic surface and via, while the capacitance C is formed due to the fringing electric fields between adjacent metal plates.

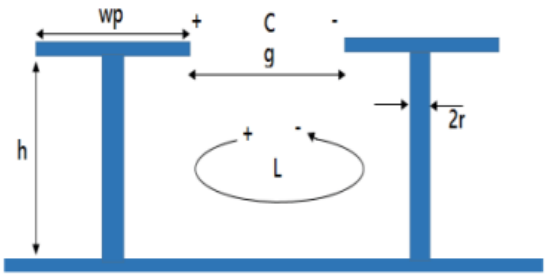

Figure 5. Equivalent electrical model.

For a conventional mushroom-like structure, the initial capacitance Cand inductance L are given by the equations below[23]:

$$L = \mu_0 \mu_r h \tag{2}$$

$$C = \frac{w\varepsilon_0(1+\varepsilon_r)}{\pi} cosh^{-1}\left(\frac{w+g}{g}\right) \tag{3}$$

where μ_0 represents the value of the free space permeability and ε_0 its permittivity.w and g represent the width of the patch and the separation between the elements of the EBG structure, respectively. The equivalent capacitance and inductance are similar to those of the conventional mushroom-like structure and the new L and C formed by the slots. By adding the slots, there is no change in the initial value of C and L, whereas the value of equivalent C and L increases and leads to a low resonant frequency and consequently a compact structure.

The associated equivalent circuit resonant frequency has the following form[23]:

$$\omega = \frac{1}{\sqrt{LC}} \tag{4}$$

The bandgap frequency bandwidth can be determined by the expression below:

$$B_w = \frac{\Delta\omega}{\omega} = \frac{1}{\eta}\sqrt{\frac{L}{C}} \tag{5}$$

where η represents the impedance of the free space.

C. The Transmission Line Method for EBG Structure Design

For obtaining a band gap characteristic of SHI structure, the transmission line based Modeling approach presented in Fig. 6 is applied. Above the rectangular SHI cells, the microstrip transmission line is positioned at a distance of 0.5mm. This line is feed by two wave reception and transmission ports [24]. The SHI cells are repeated periodically (the EBG structure is formed by 4×6 cells) and separated by g=0.36mm. The SHI structure is designed to act as a bandstop filter [25], it is built on a RogersRO3010 substrate with a surface of 40.7mm×27.3mm with a thickness equal to 1.27 mm.SHI cell sizeare optimized to obtain a WiMax band rejection around 3.5GHz.

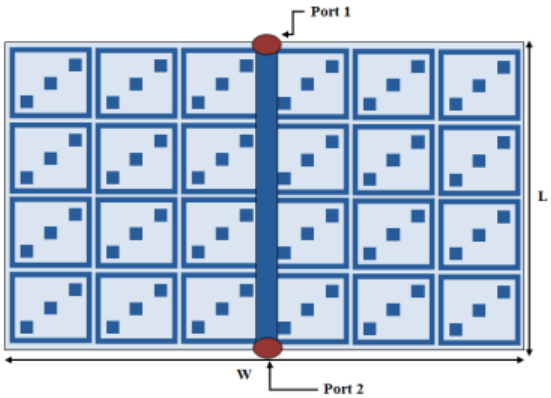

Figure 6. EBG structure: W= 40.7mm, L= 27.3mm.

The variation of the parameters S of the SHI cell is illustrated in Fig. 7. It can be noted that the S21 transmission coefficient around 3.5GHz falls below −20dB which indicates the structure's band gap behavior. It is possible to adjust the band gap width changing the dimensions of the structure.

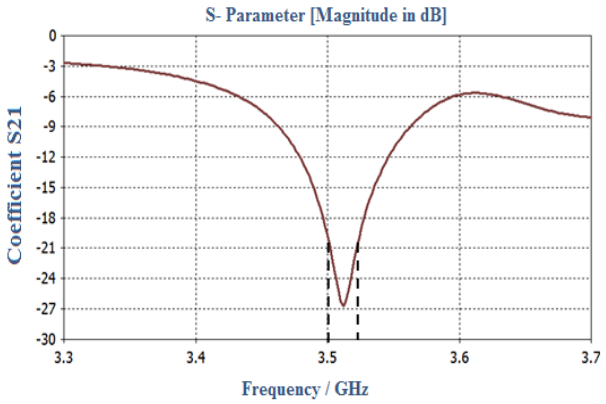

Figure 7. EBG structure transmission coefficient S21.

D. Parametric Study

Physical structure dimensions can be employed to identify EBG structure's electromagnetic properties. However, for this slotted EBG structure shown in Fig. 6, three principal parameters impacting its performance [26], which are thickness h of the substrate, its permittivity εr,

as well as superstrate effect. The impact of such parameters is studied separately in this section for the design of EBG surfaces. A trivially important effect of the vias' radius r is the fact that it is thinner than the operating wavelength.

a) Effect of substrate permittivity

Dielectric constant or permittivity of the substrate is a major factor for defining the frequency of resonance. The EBG structure analyzed in this section is presented in the Fig.6. To study the substrate permittivity effect, we varied it from 9.2 to 13.8 while keeping the other parameters the same as in Fig. 6. Fig. 8 illustrates EBG structure transmission coefficients with different permittivity's. It is observed that the EBG surface has the widest bandwidth and highest resonance, when using Rogers TMM 10 of permittivity εr = 9.2 as substrate. In other words, the bandwidth and frequency of resonance decrease while increasing the permittivity see Table II. Consequently, for the reduction of the size of EBG cells, a substrate with high dielectric constant can always be used. The price paid is a narrow bandwidth. Rogers RO3010 with a permittivity of εr= 10.2 was chosen as substrate in the rest of the simulation.

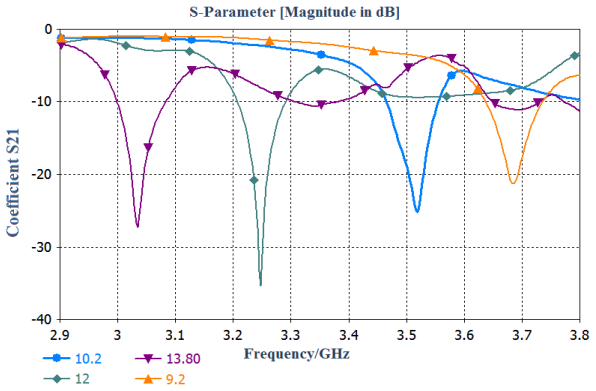

Figure 8. Effect of substrate permittivity εr on EBG structure transmission coefficient S21.

TABLE II. SUBSTRATE PERMITTIVITY EFFECT εR ON THE RESONANT FREQUENCY OF THE STRUCTURE UNDER STUDY

Permittivity εr	Frequency (GHz)	Bandwidth MHz
9.2	3.68	99.1
10.2	3.51	90
12	3.24	83.7
13.8	3.03	83

b) Substrate thickness effect

It is clear from the preceding study that the bandwidth varies with the frequency of resonance. As the frequency decreases, the bandwidth also decreases. This leads to the following question: is it feasible to simultaneously decrease the resonant frequency and increase the bandwidth? That's made through tuning the substrate's thickness h. The EBG structure analyzed is presented in Fig. 6. The thickness of the substrate h is modified from 0.5 mm to 2 mm, while the other parameters are kept.

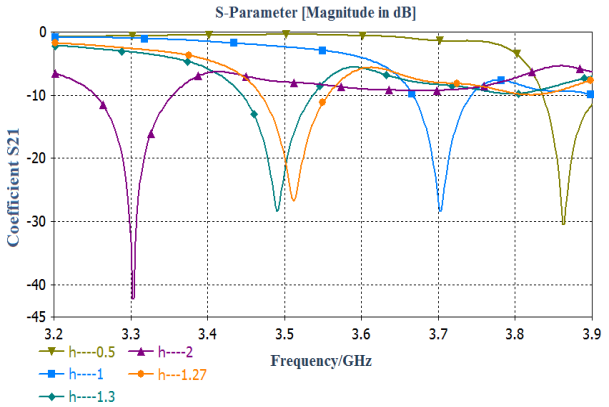

Figure 9. The impact of substrate thickness h on EBG structureS21transmission coefficient.

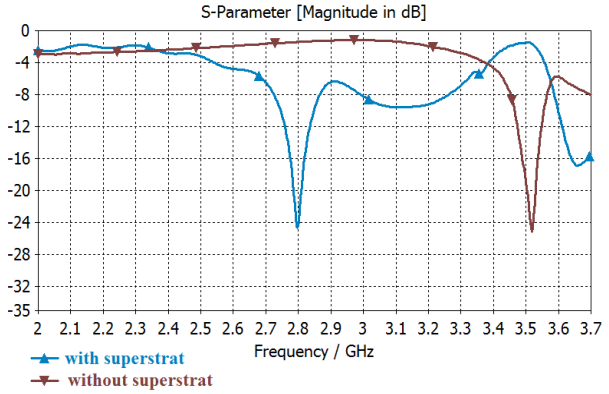

Figure 10. Substrate effect on EBG structure transmission coefficient S21.

Fig. 9 shows how the substrate thickness h affects the EBG structure's transmission coefficient S21. We observe by increasing the substrate thickness, the frequency decreases and the bandwidth increases as illustrated in Table III. The LC model also explains this. When thickness of the substrate increases, then increases the equivalent inductance L Consequently, the bandwidth increases and the frequency decreases. The thickness of h = 1.27 mm was chosen for the rest of the design. For pctical applications, a thin EBG surface is always recommended. For this reason, the thickness of the substrate should be small in comparison with the wavelength.

TABLE III. THE SUBSTRATE THICKNESS H EFFECT ON THE STUDIED EBG STRUCTURE FREQUENCY AND BANDWIDTH

Substrate thickness h(mm)	Frequency (GHz)	Bandwidth (MHz)
0.5mm	3.86	77.7
1mm	3.70	77.8
1.27mm	3.51	89.9
1.3mm	3.49	95
2mm	3.30	105

c) Effect of substrate

To protect printed antennas from environmental hazards, dielectric superstrate layers, or more popularly called cover layers, are often used. The superstrate plays a crucial role in the design of antennas, impacting several

fundamental aspects of antenna performance, including gain (as discussed in references [27, 28]), directivity (as mentioned in reference [29]), bandwidth (as outlined in reference [30]), and resonant frequency. Moreover, it also contributes to reducing mutual coupling between the radiating elements.This is clearly shown in Fig. 10, which presents the proposed EBG transmission coefficient S21 with and without a superstrate. By layering the EBG structure with a superstrate, there is a displacement of the band gaps toward a lower frequency, as illustrated in Fig. 10,which reduces the initial EBG structure size when a superstrate is not present.

E. Design of Antenna Including EBG Structure

4×6 EBG cells already presented (Fig. 6) are inserted under the dipole antenna in this section. For the design of the antenna, it is chosen a Rogers RO 3010 substrate with a relative permittivity of 10.2 and a thickness of 1.27 mm. Both the substrate and the superstrate are made of the same material. Fig. 11 shows the proposed structure's final configuration (dipole antenna with EBG).

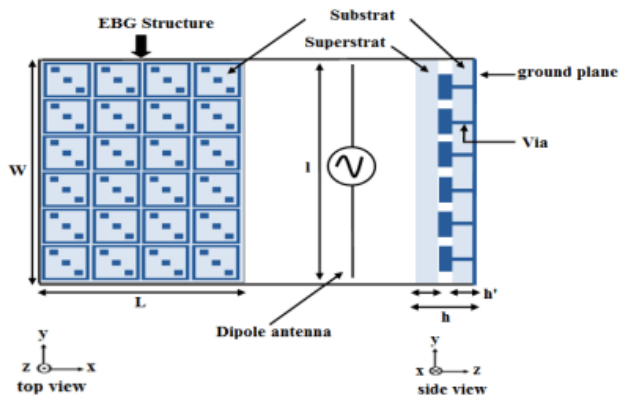

Figure 11. Design of the proposed structure: L= 27.3mm; w=40.7mm; h'=1.27mm; h=2h'+ 0.0175; g = 0.36mm; l = 38.84mm.

a) EBG unit cell type effect

The antenna design is optimized by investigating the EBG structure effect in this part. At first the mushroom-like unit cells, then EBG slotted 1, EBG slotted 2 and finally EBG Proposed are inserted separately under the dipole antenna. The reflection coefficient S11 is shown in Fig. 12 according to the different types of EBG unit cells used.

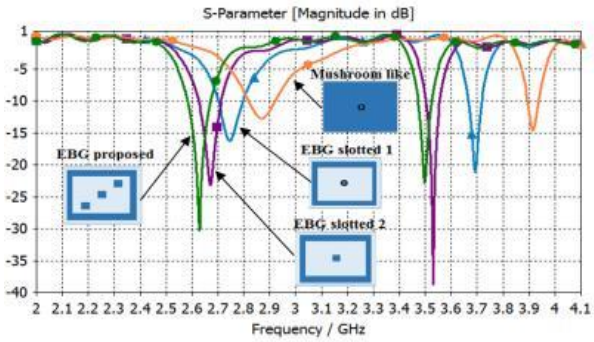

Figure 12. Dipole antenna reflection coefficients: on an EBG mushroom type structure (orange circles), EBG 1 split (blue triangles), slotted EBG 2 (purple squares), proposed EBG (green circles).

Comparing the four EBG structures in Fig. 12, it can be seen that by increasing slots in the conventional mushroom-like EBG structure, the antenna resonant frequency decreases, which means that the creation of slots results in a compact size of the structure, and also the reflection coefficient is improved. Table IV shows the comparisons between the four EBG structures.

TABLE IV. COMPARISON OF DIFFERENT TYPES OF EBGSTRUCTURES

Parameter /EBG	EBG Mushroom like	slotted EBG 1	slotted EBG 2	EBG proposed
Resonance frequency (GHz)	3.08 3.90	2.93 3.71	2.73 3.69	3.61 3.50
reflection coefficient (dB)	-23.04 -19.55	-28.04 -27.25	-38.72 -38.92	-46.72 -45.50
Percentage reduction	20 %	24 %	29 %	32 %

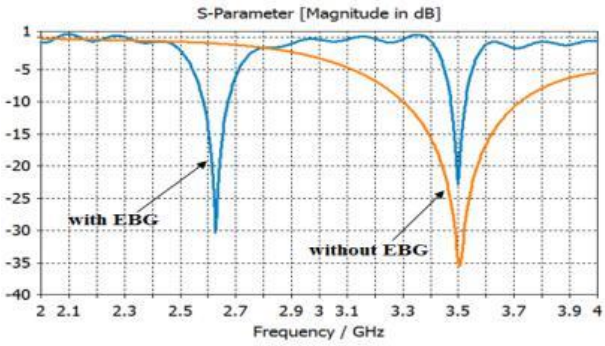

Figure 13. Antenna S parameters without and with EBG structure

From Table IV, we can see that when compared to the conventional Mushroom structure, which only reaches 20%, the proposed structure reaches the highest percentage reduction of about 32%. Therefore, a better adaptation is achieved, and hence the proposed EBG structure was chosen for the rest of the design.

The dipole antenna coefficient S11 including and excluding the EBG structure are shown in Fig.13. It is possible to observe from Fig.13, it is possible to observe another resonant frequency towards the lowest dipole antenna frequencies, leading to the double band antenna (2.6 GHz, 3.5 GHz the resonant frequency reduction from 3.5GHz to 2.6GHz allows a 32% miniaturization of the antenna size. With and without EBG structure the antenna's reflection coefficient indicates a strong match for the two different frequencies 3.5GHz and 2.6GHz.

F. Pattern of Radiation

The radiation pattern of the dipole antenna without EBG structure will be compared to that obtained using EBG structure to understand its behavior, in this simulation part. Fig. 14 and Fig. 15 show a comparison of the gain patterns of the dipole antenna with and without EBG structure at 2.6GHz and 3.5GHz resonances.

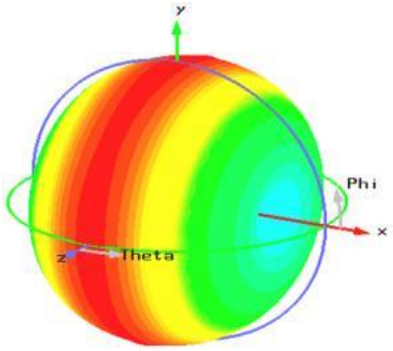

Figure 14. A conventional dipole antenna's radiation pattern in the far field at 3.5 GHz.bv ;,ko

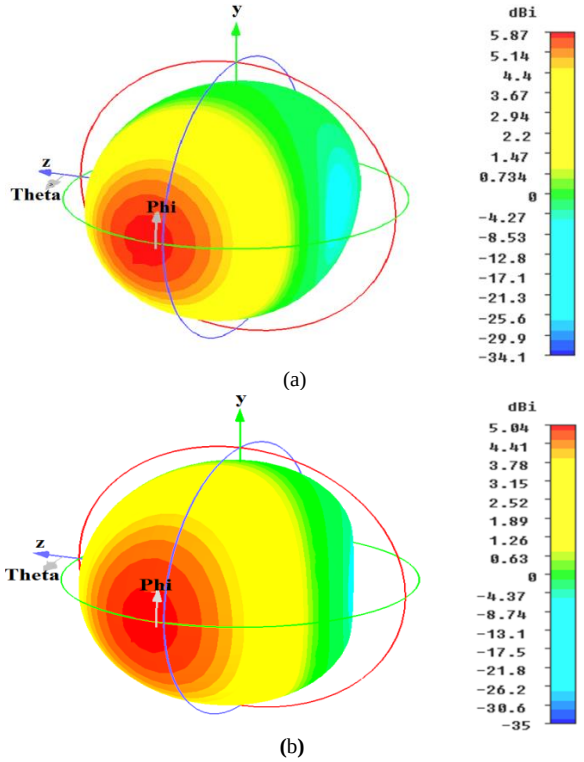

Figure 15. Radiation pattern in far field of a dipole antenna with EBG: (a) at 3.5 GHz; (b) at 2.6 GHz.

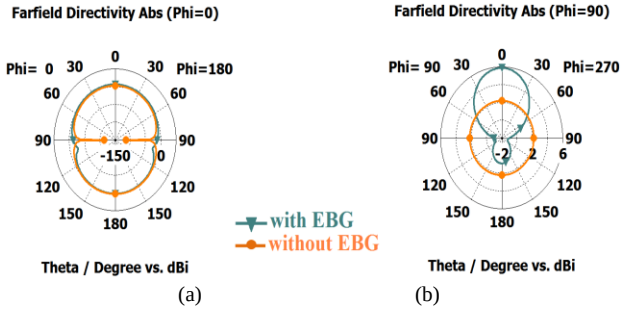

(a) (b)

Figure 16. Dipole antenna radiation pattern with and without EBG structure at 3.5GHz in the horizontal and vertical section (a) phi=0 (b) phi=90.

The directivity and gain of the conventional antenna at 3.5GHz are 2.18 dB and 2.17 dB respectively, whereas that of the dipole antenna with EBG are (5.85dB, 3.29dB) at 3.5GHz and (5.03dB, 4.91dB) at 2.6GHz respectively. Besides providing a dual band antenna and minimizing the antenna size, evidenced by a resonant frequency reduction from 3.5GHz to 2.6GHz, the performance of the antenna is improved in terms of radiation becoming directional and radiation backward is reduced, as illustrated in Figs. 16–17.

Table V summarizes the comparison of the conventional and proposed antennas. Regarding the antenna performance, it is evident that when EBG unit cells are inserted under the dipole antenna, it becomes more directive and more adapted.

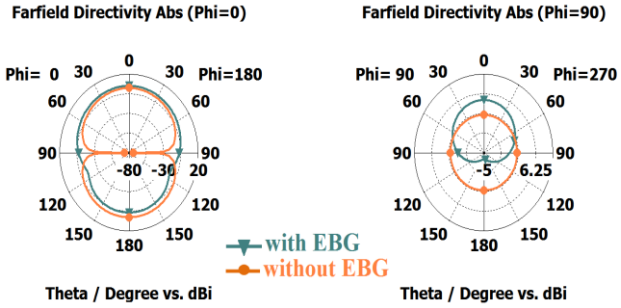

(a) (b)

Figure17. Dipole antenna radiation pattern with and without EBG structure at 2.6 GHz in the horizontal and vertical section (a) phi=0 (b) phi=90.

TABLE V. DIPOLE ANTENNA PERFORMANCE SUMMARY WITH AND WITHOUT EBG

Parameters	Dipole antenna		
	Conventional structure (without EBG)	Proposed structure (with EBG)	
Frequency (GHz)	3.5	2.6	3.5
Return Loss S11 (dB)	–40	–46.72	–45.50
Gain (dB)	2.17	5.07	3.64
directivity (dBi)	2.18	5.03	5.85
bandwidth (MHz)	580	100	65

III. PROPOSED ANTENNA REALIZATION AND MEASUREMENT

A. *The Manufacture of the Proposed Antenna*

An EBG structure combined with a dipole antenna has been designed as a prototype, simulated as well as experimentally validated for testing the proposed antenna system. Fig. 18 illustrates antenna dimensions with the proposed EBG structure. This antenna is implemented on a RO3010 substrate of 1.27 mm and 10.2 mm thickness and permittivity respectively.

The manufacturing process of the antenna is divided into three main parts:

- Welding of two rods for the dipole antenna.
- Fabrication of the EBG structure using the LPKF protolaser U4 printed circuit board engraving machine.
- Bonding the substrate containing the EBG with the superstrate.
- Deposition of the dipole antenna 1.5 mm above the EBG structure.
- Prototype measurement is carried out using a Vector Network Analyzer (VNA) - ROHDE & SCHWARZ ZVB20

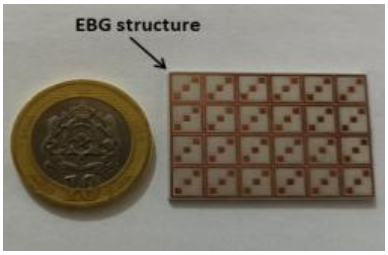

(a)

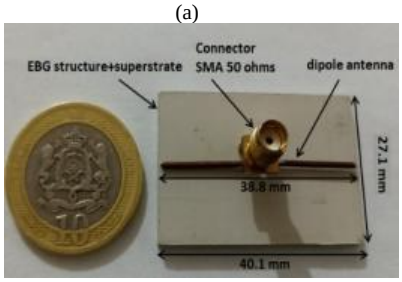

(b)

Figure 18. Dimensions of the proposed antenna: (a) EBG structure used (b) proposed dipole antenna

B. The Proposed Antenna's Reflection Coefficient Measurement

Fig. 19 shows a setup used for S11 (dB) measurement of the antenna. The results of the simulation and measurement for the proposed antenna are shown in Fig.20.

The Fig.20 shows a slight discrepancy between the simulation results and the experimental measurements. This difference is attributable to the fact that during the fabrication of the antenna, it was not possible to achieve a perfect bonding between the superstrate and the substrate, resulting in the presence of a slight gap between them.

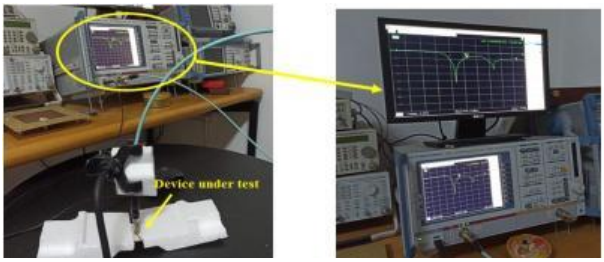

Figure 19. Setup used for measuring S11 (dB) of the proposed dipole antenna.

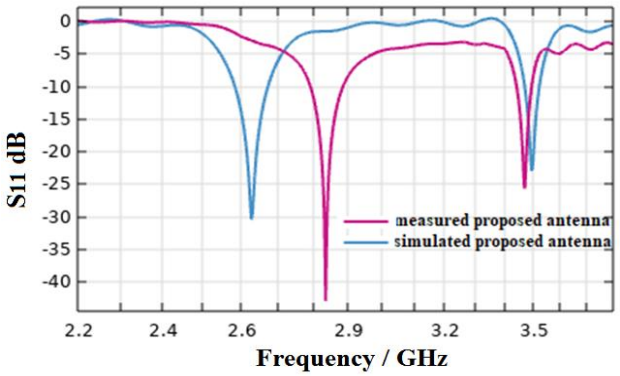

Figure 20. Experimentally measured S11 coefficient using the VNA Compared with simulated S11

Table VI presents a summary of the parameters of the proposed antenna with respect to the different configurations of the antenna described in [22, 24–27]. From the study carried out, it is clear that our design has the smallest volume among all the designs. The benefits and novelty of ourproposed design lay in the ability to operate simultaneously in two frequencies of the sub-6 GHz 5G bands, 3.5 GHz and 2.6 GHz with a low profile.

TABLE VI. PROPOSED ANTENNA COMPARED TO OTHER WORK

References	Employed techniques	Resonance frequency GHZ	Gain dBi	Antenna size (mm^2)
This work	EBG structure - Superstrate	2.6–3.5	4.91–3.29	40.7×27.3
Pant*et al.* [15]	RF PIN Diode	2.2–2.7 3.3–4.02	3.7 dBi at 2.7 GHz	120 × 60
Lee and Jang [16]	SP4T Switch	2.5–3.6	1.9 dBi at 3.5 GHz	100×60
Yang *et al.* [17]	RF PIN Diode	2.4–2.7 3.4–3.6	7.41dBi at 3.5GHz	100×100
Gohar*et al.* [31]	MTM -Fractals	3.15–4.56	3.5–2.6	40×40
Juan*et al.* [32]	Capacitive Loading	3.33–3.63	6.4–6.57	51×51
Mohammadsadegh *et al.* [33]	loaded with a via-less MTM	2.332 4.02 5.23	2.23 2.81 1.91	60 × 40
Rezvani and Zehforoosh [34]	metamaterial structure	2.4–3.1 5.1–5.8	5 6	180×90
Han*et al.* [35]	Slot antenna with Two PIN diodes	3.4–3.8 3.7–4.2	2.24 2.76	40×30

IV. CONCLUSION

A novel conception of a dual-band antenna using an EBG electromagnetic band spacing structure has been simulated and fabricated in this paper. By introducing EBG electromagnetic bandgap structures below the conventional dipole antenna, previously operating at only one frequency of 3.5 GHz, two resonant frequencies (3.5 GHz and 2.6 GHz) have been obtained. High radiation characteristics are achieved at each resonance frequency, providing a significant improvement in directivity and

gain. Moreover, this technique reduces the proposed antenna size by 32%, consequently, due to its small size, it can be easily incorporated in applications of modern wireless communication.The implications of these results offer promising prospects for future research, particularly regarding multiband antenna design and antenna size reduction.

CONFLICT OF INTEREST

The authors declare no conflict of interest.

AUTHOR CONTRIBUTIONS

Sara Said conducted the research under the supervision of AbdenacerEssalhi. Abdelhafid Messaoudi and Kamal Kassmi carried out the practical part, validated by Kaabal Abdelmoumen. Faize Ahmed and Baghazelhadi checked the article. All authors approved the final version.

REFERENCES

[1] F. Yang and Y. R. Samii, *Electromagnetic Band Gap Structures in Antenna Engineering*, Cambridge University Press Cambridge, UK, pp. 1–5, 2009.

[2] A. V. kavokin, J. J. Baumberg, G. Malpuech, and F. P. Laussy,*Microcavities*, Oxford University Press, vol. 21, 2017.

[3] R. Coccioli, F.R. Yang, K.P. Ma, and T. Itoh, "Aperture-coupled patch antenna on UC-PBG substrate," *IEEE Trans. on Microwave Theory and Techniques*, vol. 47, no 11, pp. 2123–2130, Nov.1999.

[4] J. S. Colburn and Y. R. Samii, "Patch antennas on externallyperforated high dielectric constant substrates," *IEEE Trans. on Antennas and Propagation*, vol. 47, no 12, pp. 1785–1794, 1999.

[5] S. Said, A. Es-salhi, and M. Elhitmy, "Reduction of mutual coupling betweenradiating elements of an array antenna using EBG electromagnetic band structures," *International Journal of Electrical and Electronic Engineering &Telecommunications*, vol. 10, no. 2, pp. 91–98, Mar.2021.

[6] B. Mohamadzade, A. Lalbakhsh, R. B. V. B. Simorangki*et al.*, "Mutualcouplingreduction in microstriparrayantenna by employingcutside patches and EBG structures," *Progress in ElectromagneticsResearch M*, vol. 89, pp. 179–187, Jan.2020.

[7] A. H. Abdelgwad and M. Ali, "Isolation improvementbetweenclosely-spacedantennasusing EBG," in *Proc. of 2020 International AppliedComputationalElectromagnetics Society Symposium*,pp. 1–2, 2020

[8] A. Rahman*et al.*,"Design of a 5G Sub-6 GHz vehicular cellular antenna element with consistent radiation pattern using characteristic mode analysis," *Sensors*, vol. 22, no 22, p. 8862, 2022.

[9] X.Li*et al.*,"A low-profile wide bandphased array antenna using EBG structures in P-band," in *Proc. of 2019 IEEE Int. Conf. on ComputationalElectromagnetics*,pp. 1–3,2019.

[10] M. S. Kanitkar, S. B. Deosarkar, and K. R. Joshi, "Design of frequency reconfigurable antennausing dual band elec-tromagnetic band gap structure," *Indian Journal of Science and Technology*, vol. 13, no 30, pp. 3041–3050, 2020.

[11] T. A. Elwi, "A slotted lot us shapedmicrostripantennabased on EBG structure," *Journal of Material Sciences and Engineering*, vol. 7, no. 2, p.439, 2018.

[12] D.Singh, A.Thakur, and V.M.Srivastava,"Miniaturization and gain enhancement of microstrip patch antenna using defected groundwith EBG," *J. Commun.*, vol. 13, no 12, pp. 730–736, 2018.

[13] X. Shen, Y. Liu,L. Zhao, G. L.Huang, X. Shi, and Q. Huang, "A miniaturizedmicrostripantennaarray at 5G millimeter-waveband," *IEEE Antennas and Wireless Propagation Letters*, vol. 18, no 8, pp. 1671–1675, Aug.2019.

[14] T. O. Olawoye andP. Kumar, "A high gain antenna with DGS for sub-6 GHz 5G communications," *Advanced Electromagnetics*, vol. 11, no. 1, p. 41–50, 2022.

[15] A. Pant, M. Singh, M., and M. S. Parihar, "A frequency reconfigurable/switchable MIMO antenna for LTE and early 5G applications," *AEU-International Journal of Electronics and Communications*, vol. 131, Mar. 2021

[16] W.-W. Lee and B. Jang, "A tunable MIMO antennawith dual port structure for mobile phones," *IEEE Access*, vol. 7, pp. 34113–34120, Mar. 2019.

[17] G. Jin, C. Deng, J. Yang *et al*., "A new differentially-fed frequency reconfigurable antenna for WLAN and sub-6GHz 5G applications," *IEEE Access*, vol. 7, pp. 56539–56546, Feb. 2019.

[18] Z. Raida, D. Černohorský, D. Gala *et al*.Multimediálníučebnice: Elektromagnetickévlny, Mikrovlnnátechnika. [Online]. Available:http://www.urel.feec.vutbr.cz/~raida/multimedia/index.php

[19] G. K. Pandey, H. S. Singh, P. K. Bharti, and M. K. Meshram, "Design of WLAN band notched UWB monopole antennawithstepped geometryusingmodified EBG structure," *Progress in ElectromagneticsResearch B*, vol. 50, pp. 201–217, Apr.2013.

[20] L. Yangjn, M. Fan, F. Chen, J. She, and Z. Feng, "A novel compact electromagneticbandgap (EBG) structure and its applications for microwave circuits," *IEEE Trans. on Microwave Theory and Techniques*, vol. 53, no. 1, pp. 183–190, Jan.2005.

[21] Z. Iluz, R. Shavit, and R. Bauer, "Microstripantennaphasedarraywithelectromagneticbandgapsubstrate," *IEEE Trans on Antennas and Propagation*, vol. 52, no. 6, pp. 1446–1453, June.2004.

[22] Y. Kim, F. Yang, and A. Elsherbeni, "Compact artificialmagneticconductor designs usingplanar square spiral geometries," *Progress in ElectromagneticsResearch*, vol. 77, pp. 43–54, Aug.2007.

[23] D. F. Sievenpiper, *High-Impedance Electromagnetic Surfaces*, Ph.D. dissertation at Universityof California, Los Angeles, pp. 1–24, 1999

[24] M. S. Alam, M. T. Islam, and N. Misran, "A novel compact split ring slottedelectromagneticbandgap structure for microstrip patch antenna performance enhancement," *Progress in ElectromagneticsResearch*, vol. 130, pp. 389–409, Aug.2012.

[25] A. Kaabal, S. Ahyoud, and A. Asselman, "A new design of star antenna for ultra-wide band applications with WLAN-band-notchedusing EBG structures," *Int. J. MicrowOpt. Technol*., vol. 9, pp. 544–548, Sept.2014.

[26] E. Yablonovitch, "Inhibitedspontaneousemission in solid-state physics and electronics," *Phys. Rev. Lett.*, vol. 58, pp. 2059–2063, May.1987.

[27] M. Fanji and S. K. Sharma, "A dual-band high-gain resonantcavityantennawitha single layer superstrate," *IEEE Trans AntennasPropag*., vol. 63, no. 5, pp. 2320-2325, May.2015.

[28] B. A. Arand and A. Bazrkar, "Gain enhancement of a tetra-band square-loop patch antennausing an AMC–PEC substrate and asuperstrate," *Wireless Personal Communications*, vol. 84, no 1, pp. 87–97, Apr.2015.

[29] H. Xu, Z. Zhao, Y. Lv, C. Du, and X. Luo, "Metamaterialsuperstrate and electromagnetic band-gap substrate for high directive antenna," *International Journal of Infrared and MillimeterWaves*, vol. 29, no. 5, pp. 493–498,Mar. 2008.

[30] F. H. Wee, F. Malek, A. U. Al-Amaniet al., "Effect of twodifferentsuperstratelayers on bismuth titanate (BiT) arrayantennas," *Scientific Reports*, vol. 4, no 1, pp. 1–8, Jan.2014.

[31] V. Gohar, K. Asghar, D. Navid*et al*.,"Microstripsierpinskifractal carpet for slot antennawithmetamaterialloads for dual-band wireless application," *AEU-International Journal of Electronics and Communications*, vol. 84, pp. 93–99, Feb. 2018.

[32] Y. Juan, W. Yang, and W. Che, "Miniaturizedlow-profile circularlypolarizedmetasurfaceantennausing capacitive loading," *IEEE Trans on Antennas and Propagation*, vol. 67, no 5, pp. 3527–3532, May.2019.

[33] K. Mohammadsadegh, Z. Ehsan, B. Raheleh, and V. Mashayekhi, "Miniaturized triple-band monopole antennaloadedwith a via-less MTM for 3G, WIMAX, and WLAN applications," *International Journal of Microwave and Wireless Technologies*, pp. 601–608, May 2021.

[34] M. Rezvani and Y. Zehforoosh, "A dual-band multiple-input multiple-output microstripantennawithmetamaterial structure for

LTE and WLAN applications," *AEU-International Journal of Electronics and Communications*, vol. 93, pp. 277–282, Sept.2018.
[35] L. Han, C. Wang, W. Zhang, R. Ma, and Q. Zeng, "Design of frequency-and pattern-reconfigurable wideband slot antenna," *International Journal of Antennas and Propagation*, pp.1–7,2018.